Biochemical Pharmacology, Vol. 60, pp. 571–579, 2000.


ISSN 0006-2952/00/$–see front matter
PII S0006-2952(00)00346-4

# Reductive Activation of Mitomycin C by Neuronal Nitric Oxide Synthase

*Hou-Bo Jiang,* Minoru Ichikawa,† Aizo Furukawa,* Shuhei Tomita* and Yoshiyuki Ichikawa*‡*

*Department of Biochemistry, Kagawa Medical University, Kagawa 761-0793, Japan; and †Division of Cellular Genetics, Institute for Molecular and Cellular Biology, Osaka University, Osaka 565-0871, Japan

**ABSTRACT.** Mitomycin C (MC) requires bioreduction prior to the generation of alkylating moieties. NADPH-cytochrome P450 reductase is predominant in metabolic activation of MC in hypoxic cancer cells. In this study, neuronal nitric oxide synthase (nNOS), whose reductase domain is structurally similar to that of NADPH-cytochrome P450 reductase, was assessed for its ability to activate MC. nNOS under anaerobic conditions catalyzed the reduction of MC, which was measured as the decrease in absorbance at 375 nm. Neither the heme blocker potassium cyanide (1 mM) nor the nNOS competitive inhibitor $N^G$-nitro-L-arginine methyl ester (L-NAME, 1 mM) affected the bioreduction of MC, whereas 0.1 mM diphenyleneiodonium chloride, which binds to the reductase domain of nNOS, inhibited MC reduction completely. The reduction of MC by nNOS was influenced by $Ca^{2+}$/calmodulin. In the absence of $Ca^{2+}$/calmodulin, the rate of MC reduction decreased by 28% at pH 6.6. The formation of an alkylated complex of 4-(*p*-nitrobenzyl)pyridine occurred in a manner analogous to that observed in MC metabolic experiments. The rate of MC reduction and the formation of the alkylated complex of 4-(*p*-nitrobenzyl)pyridine at pH 6.6 were increased by 43 and 54%, respectively, as compared with that at pH 7.6. nNOS-activated MC resulted in the consumption of oxygen in air. The rate of oxygen consumption decreased by 50% in the presence of 2000 U/mL of catalase. MC inhibited nNOS activity in a noncompetitive manner. These findings demonstrate that nNOS is capable of catalyzing the bioreduction of MC. BIOCHEM PHARMACOL **60**;4:571–579, 2000. © 2000 Elsevier Science Inc.

**KEY WORDS.** mitomycin C; reduction; metabolic activation; neuronal nitric oxide synthase; antitumor activity

MC§ is an important active drug commonly used in combination chemotherapy regimens to treat breast, lung, prostate, and colorectal cancers, and is probably the drug of choice for intravesical administration in superficial bladder cancer [1]. MC is a prototype bioreductive alkylating agent, which requires enzymatic activation prior to the generation of alkylating moieties [2]. The first stage in the activation of MC is quinone reduction, which can be catalyzed by several different enzymes. These include NADPH:cytochrome P450 oxidoreductase (EC 1.6.2.4) [3, 4], xanthine:oxygen oxidoreductase (EC 1.2.3.2; xanthine oxidase) [3, 5], and NADH:ferricytochrome $b_5$ oxidoreductase (EC 1.6.2.2; cytochrome $b_5$ reductase) [6], acting as one-electron reductases, and xanthine:$NAD^+$ oxidoreductase (EC 1.2.1.37; xanthine dehydrogenase) [7, 8] and NAD(P)H:quinone oxidoreductase (EC 1.6.99.2; DT-diaphorase) [9], acting as two-electron reductases. All the major enzymes involved in MC bioreduction exhibit very low Michaelis–Menten affinity constants for MC, suggesting that no one reductase should show a preference for MC as a substrate. NADPH-cytochrome P450 reductase and DT-diaphorase are believed to predominate in metabolic activation of MC in hypoxic cancer cells and in normally oxygenated cells, respectively [9, 10]. However, more recent experiments with xenografts have indicated that metabolic activation of MC occurs *in vivo* predominately under hypoxic conditions [11]. It also has been suggested that other undetermined enzymes may be involved in the metabolic activation of MC [12–14].

NOS (EC 1.14.13.39) catalyzes the NADPH-dependent oxidation of L-arginine to nitric oxide and L-citrulline [15]. Three NOS isoforms have been characterized. Two constitutive forms have been identified in the cerebellum (nNOS) [16] and endothelial cells (eNOS) [17], respectively. An inducible form (iNOS) is expressed in response to lipopolysaccharide and cytokines in a large variety of cells [18]. The three isoforms, exhibiting structural similarity, are homodimers in their active forms, and each subunit

‡ Corresponding author: Dr. Yoshiyuki Ichikawa, Department of Biochemistry, Kagawa Medical University, Miki-cho, Kita-gun, Kagawa 761-0793, Japan. Tel. and FAX (81) 87-891-2105; E-mail: hjiang@kms.ac.jp

§ *Abbreviations*: MC, mitomycin C; NOS, nitric oxide synthase; nNOS, neuronal NOS; eNOS, endothelial NOS; iNOS, inducible NOS; SOD, superoxide dismutase; L-NAME, $N^G$-nitro-L-arginine methyl ester; $BH_4$, tetrahydrobiopterin; DPI, diphenyleneiodonium chloride; and PNBP, 4-(*p*-nitrobenzyl)pyridine.

Received 25 October 1999; accepted 21 January 2000.

comprises a C-terminal reductase domain and an N-terminal oxygenase domain [19, 20]. The reductase domain contains the binding sites for FMN, FAD, and NADPH, and is responsible for transferring electrons from NADPH to the oxygenase domain [20]. The oxygenase domain contains the binding sites for tetrahydrobiopterin, L-arginine, and heme, and is responsible for maintaining the active dimeric structure and catalyzing NO synthesis [15]. Calmodulin binds to a region between the two domains, and is thought to activate electron transfer between the two domains [21].

NOS isoforms have been shown to be expressed in N1E-115 neuroblastoma cell lines [22], human colon cancer cell lines [23], and the human cervix carcinoma cell line ME-180 [24]. Recently, an increased level of nNOS and eNOS expression has been found in human central nervous system tumor cells and tumor endothelial cells, respectively [25]. High-level expression of iNOS has been shown in human colon adenomas [26], breast tumors [27], and ovarian tumors [28]. nNOS has also been indicated to be expressed in vascular endothelial and myoepithelial cells in breast tumors [27].

The reductase domains of NOS isoforms have been shown to have enzymatic activities similar to that of NADPH-cytochrome P450 reductase, and they have been suggested to participate in the cellular electron transfer process [29]. Taking into consideration that NADPH-cytochrome P450 reductase plays a predominant role in metabolic activation of MC [3, 4], and that nNOS catalyzes quinone reduction in 7-ethoxyresorufin [30], it was of interest to determine whether or not NOS isoforms are involved in the bioreduction of MC.

For this reason, we expressed active nNOS in *Escherichia coli* and purified nNOS. The ability of nNOS to metabolize MC was assessed by measuring MC reduction and the formation of an alkylated complex of 4-(*p*-nitrobenzyl)pyridine under aerobic and anaerobic conditions. Since activation of MC by various reductases appeared to be dependent upon the pH, the effect of pH on the reduction of MC by nNOS was also examined.

## MATERIALS AND METHODS

### *Materials*

SOD (from bovine erythrocytes), catalase, L-NAME, cytochrome *c* (from horse heart), and $BH_4$ were obtained from the Sigma Chemical Co. NADPH was purchased from the Oriental Yeast Co. MC, L-arginine, sodium ampicillin, sodium tetracycline, DPI, and PNBP were from Wako Pure Chemicals. 2′,5′-ADP-Sepharose and calmodulin-Sepharose 4B were from Pharmacia LKB Biotechnol. Bradford protein assay kits were from Bio-Rad. Nitrogen gas was purchased from the Nippon Sanso Co., its purity being more than 99.8%.

Absorption spectra were recorded with a Beckman DU-640 spectrophotometer (Beckman Instruments Inc.), and were transferred to a Macintosh computer for analysis and display. The cuvette containing a sample was placed in a temperature-controlled cell holder.

### *Plasmid Construction*

The mouse nNOS expression plasmid, pCW-nNOS, was constructed as follows. Mouse nNOS/pSG5 containing full-length mouse nNOS cDNA was used to construct a prokaryotic expression system [31]. Polymerase chain reaction (PCR) was used to amplify the region of nNOS cDNA between the initiator methionine and the internal *Bam*HI restriction site of mouse nNOS/pSG5. This allowed the introduction of a unique *Nde*I site for cloning purposes. The product was ligated into the pGEM-T easy vector (Promega), and then into mouse nNOS/pSG5 using the *Eco*RI and *Bam*HI restriction sites. The gene was cloned into the pCW vector using the *Nde*I and *Xba*I restriction sites to give pCW-nNOS, which was cotransformed with pGroELS into *E. coli* BL21.

### *nNOS Expression*

Flasks containing 1 L of modified Terrific Broth, 50 μg/mL of ampicillin, and 10 μg/mL of tetramycin were inoculated with 10 mL of an overnight culture (grown in LB), and then shaken in the dark at 220 rpm at 37°. The cultures were grown to an $OD_{600}$ of 0.6 to 0.7, and then the heme and flavin precursors, δ-aminolevulinic acid and riboflavin, were added to final concentrations of 500 and 3 μM, respectively. Protein expression was induced at $OD_{600}$ = 1.0 to 1.4 by the addition of isopropyl-β-d-thiogalactoside to 1 mM. Since pGroELS was present, 1 mM ATP was also added. The cells were incubated for 40 hr after induction with shaking at 220 rpm at 22°, and then harvested and frozen at −80° until purification.

### *nNOS Purification*

Harvested cells were resuspended in homogenization buffer, lysed by pulsed sonication (1 min, 50% power, three times), and then centrifuged at 150,000 *g* for 60 min to sediment the cell debris. The supernatant was applied to a 2′,5′-ADP-Sepharose column equilibrated with the same buffer. The column was washed extensively, and then the protein was eluted with 5 mM 2′-AMP. The nNOS-containing fractions were pooled and concentrated (Centriprep 30, Amicon). L-Arginine and $BH_4$ were added to final concentrations of 2 and 1 mM, respectively, followed by overnight incubation at 4° and loading onto a calmodulin-Sepharose 4B column. Finally, the nNOS was eluted with 5 mM EDTA. The eluted nNOS was concentrated, aliquoted into small vials, and then quickly frozen. The enzyme was stored at −80° until used.

The purified nNOS was analyzed by SDS–PAGE. The proteins were transferred to a polyvinylidene difluoride membrane (Millipore), which later was incubated with

anti-nNOS antibody (Transduction Laboratories) and then with horseradish peroxidase-conjugated anti-rabbit IgG.

### *Determination of NOS Activity*

NOS activity was determined at 37° using a spectrophotometric oxyhemoglobin assay for NO [32]. One to two micrograms of purified nNOS was added to a cuvette containing 10 mM potassium phosphate, pH 7.6, 10 μM oxyhemoglobin, 0.5 mM dithiothreitol (DTT), 4 μM each of FAD and FMN, 10 μM $BH_4$, 100 μM L-arginine, 1 mM $Ca^{2+}$, 17.7 μg/mL of calmodulin, and 0.1 mM NADPH, in a final volume of 1 mL. In the kinetic studies, the L-arginine concentration was varied from 2 to 40 μM in the presence of various concentrations of MC dissolved in 70% (v/v) aqueous ethanol. Reactions were started by the addition of NADPH. The NO-mediated conversion of oxyhemoglobin to methemoglobin was monitored at 37° as the increase with time in absorbance at 401 nm, and the nNOS activity was quantitated using an extinction coefficient of 38 $mM^{-1}$ $cm^{-1}$. The MC concentration was calculated with an extinction coefficient of 21.8 $mM^{-1}$ $cm^{-1}$ at 367 nm [3].

### *Reduction of Cytochrome c by nNOS*

The reduction of cytochrome *c* by nNOS was examined spectrophotometrically at 550 nm using an extinction coefficient of 21 $mM^{-1}$ $cm^{-1}$ [33]. The enzymatic reaction mixtures contained 1–2 μg nNOS, 10 mM potassium phosphate, pH 7.6 or 6.6, 4 μM each of FAD and FMN, 100 U/mL of SOD, 10 U/mL of catalase, 0.6 mM $Ca^{2+}$, 17.7 μg/mL of calmodulin, and 100 μM cytochrome *c*, in a total volume of 1 mL. Each reaction mixture was preincubated for 5 min at 25° to oxidize residual DTT and $BH_4$ carried over in the enzyme aliquot, and then the reaction was started by the addition of 200 μM NADPH. NADPH addition to the cuvette did not increase its final volume by more than 5%.

### *Reduction of MC by nNOS*

The relative rates of MC reduction were determined in reaction mixtures containing 10 mM potassium phosphate, pH 6.6 or 7.6, 4 μM each of FAD and FMN, 1 mM $Ca^{2+}$, 17.7 μg/mL of calmodulin, 20 μM NADPH, various concentrations of nNOS, and 50 μM MC, in a final volume of 2 mL. The enzymatic reactions were started by the addition of NADPH. MC was dissolved in 70% aqueous ethanol. The maximum final concentration of ethanol in the assay mixtures was 0.2% (v/v). The reduction of MC was measured as the decrease in absorbance at 375 nm (extinction coefficient, 13.2 $mM^{-1}$ $cm^{-1}$) at 25° under anaerobic conditions [34]. Anaerobic measurement of the reduction of MC was performed as follows: cuvettes containing reaction mixtures without NADPH were made anaerobic by repeated cycles of evacuation and equilibration with catalyst-deoxygenated nitrogen. The NADPH solution was evacuated and purged with nitrogen gas in a separate vessel. NADPH was transferred with gas-tight syringes to the cuvettes to start the enzymatic reaction, and the cuvettes were maintained under positive pressure during spectrophotometric measurements.

### *Alkylation Studies*

The generation of alkylating metabolites of MC by nNOS was assayed by means of a previously reported method [6]. The reaction mixture contained 3 mM NADPH, 0.1% PNPB dissolved in acetone, 0.3 mM MC, 4 μM each of FAD and FMN, 1 mM $Ca^{2+}$, 17.7 μg/mL of calmodulin, 0.075 nmol nNOS, and 10 mM potassium phosphate, pH 6.6 or 7.6, in a total volume of 1 mL. Under subdued light, the reaction tubes were warmed for 10 min at 37°, the reaction being started by the addition of MC, which was dissolved in 50% aqueous acetone. The final concentration of acetone, used to solubilize the MC and PNBP, in the reaction mixture was 2%, which had no effect on the enzyme-catalyzed bioactivation of MC. The reactions were conducted for 30 min at 37°. Hypoxia was accomplished by sealing the tubes with rubber septa fitted with 18-gauge (inflow) and 21-gauge (outflow) needles, and by pregassing the reaction mixtures during the 10-min warming step with humidified nitrogen gas containing less than 10 ppm oxygen. Hypoxia was maintained with a continuous flow of nitrogen during the course of the reaction. MC was added, without interrupting the hypoxia, by injection in a 10 μL volume through the septa. Aerobic tubes were also sealed after the addition of MC to prevent evaporation, but were not gassed. After incubation, the tubes were placed on ice, the septa were removed, and the reaction was terminated by the addition of 2 mL of reagent-grade acetone. Color was developed by the addition of 1 mL of 1 M sodium hydroxide, and the colored PNBP-MC adduct was extracted immediately with 4 mL of HPLC-grade ethyl acetate. The phases were separated by centrifugation for 2 min at 1000 *g*, and then the absorbance at 540 nm of the ethyl acetate phase was determined spectrophotometrically.

### *Determination of Oxygen Consumption*

The oxygen concentration was determined with a Gilson model 5/6H oxygraph (Gilson Medical Electronics) equipped with a Clark electrode. The enzymatic reactions were performed in 10 mM potassium phosphate, pH 7.6, with 4 μM each of FAD and FMN, 1 mM $Ca^{2+}$, 17.7 μg/mL of calmodulin, 200 μM NADPH, 0.1 nmol nNOS, and various concentrations of MC, in a final volume of 2 mL at 37°. The concentration of molecular oxygen in distilled water was estimated to be 197 μM, assuming 100% saturation at 37° in a 21% oxygen atmosphere.

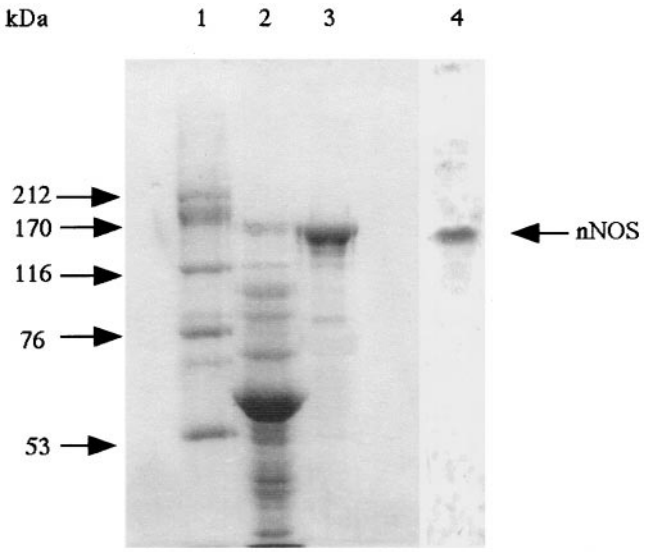


**FIG. 1. SDS–PAGE and western blot analysis of purified nNOS isolated from *E. coli*. Lane 1, molecular weight standards; Lane 2, crude cell lysate (18 μg); Lane 3, purified nNOS (3.5 μg). The 7.5% polyacrylamide gel has been stained with Coomassie blue. Lane 4, purified nNOS analyzed by western blotting with an anti-nNOS antibody. The purified nNOS ran as a band of 160 kDa.**

### *Protein Content Determination*

The protein content was determined by the method of Bradford (Bio-Rad Protein Assay Kit) with BSA as the standard protein. The concentration of nNOS was determined from the optical spectrum of nNOS using the extinction coefficient, $\Delta\epsilon_{(444-475nm)} = 75\ mM^{-1}\ cm^{-1}$, for the ferrous-CO complex [35].

### *Statistical Analysis*

Data are expressed as means ± SEM for the indicated numbers of experiments. Statistical analyses were performed using Student's *t*-test. The 0.05 level of statistical significance was used in all experiments.

## RESULTS

### *Characterization of nNOS Expressed in* E. coli

The co-expression of nNOS with the *E. coli* groE molecular chaperonin system (groEL and groES) and growth of the cells at a low temperature (22°) resulted in overexpression of functional nNOS. The expressed nNOS was purified by two sequential affinity chromatographic steps on a 2′,5′-ADP-Sepharose and a calmodulin-Sepharose 4B column. The purified nNOS was determined to be greater than 90% pure by SDS–PAGE and was confirmed by western blotting with anti-nNOS antibody (Fig. 1). The purified nNOS ran as a prominent band of 160 kDa on SDS–PAGE. Typically, the procedure produces 10–15 mg nNOS/L of *E. coli* culture.

The recombinant nNOS was active with a $V_{max}$ of 425 ± 13 nmol $min^{-1}$ $mg^{-1}$ protein and a $K_m$ of 2.56 ± 0.13 μM at 37°. The activity of the recombinant nNOS was dependent on $Ca^{2+}$/calmodulin: 320 ± 17 nmol $min^{-1}$ $mg^{-1}$ with $Ca^{2+}$/calmodulin versus 21 ± 3 nmol $min^{-1}$ $mg^{-1}$ without. Furthermore, the activity of the enzyme was enhanced by 2-fold in the presence of exogenous $BH_4$. However, the enzymatic activity was inhibited completely by 1 mM L-NAME. These values are in excellent agreement with those reported previously for native nNOS [16].

### *Metabolic Reduction of MC by nNOS*

nNOS was capable of catalyzing the reduction of MC, which was measured spectrophotometrically as the decrease in absorbance at 375 nm. As shown in Fig. 2A, MC

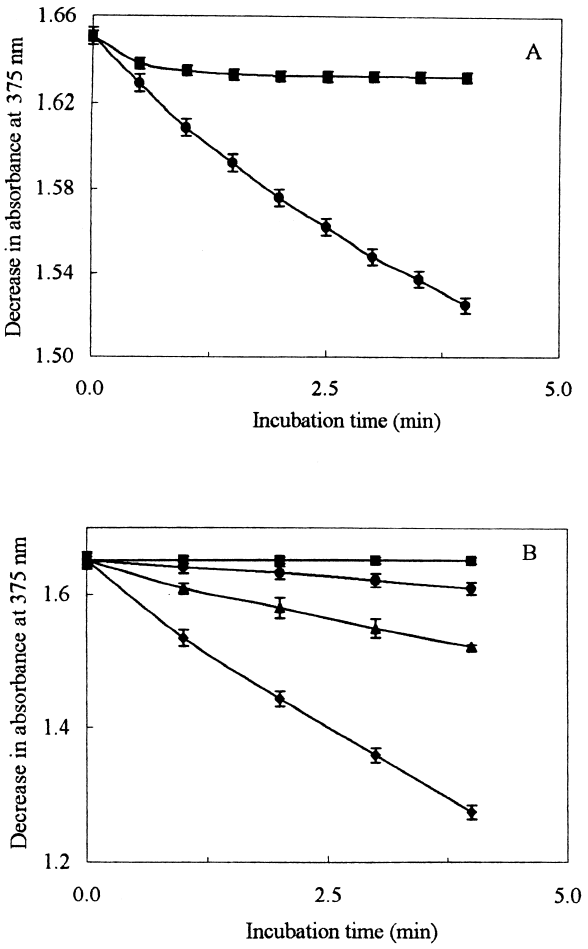


**FIG. 2. Reduction of MC by nNOS. (A) Reduction of MC by nNOS under aerobic (squares) and anaerobic (circles) conditions. The reaction mixture consisted of 50 μM MC, 20 μM NADPH, 0.0125 nmol purified nNOS, and 10 mM potassium phosphate, pH 7.6, in a total volume of 1 mL. (B) Effect of nNOS concentration on the rate of MC reduction under anaerobic conditions. The reaction mixture was the same as in panel A except for the nNOS concentration. Squares, pre-boiled nNOS; circles, 0.0075 nmol nNOS; triangles, 0.0125 nmol nNOS; and diamonds, 0.0175 nmol nNOS. The reduction of MC is expressed as the decrease in absorbance at 375 nm. Data are expressed as means ± SEM for five determinations.**

**TABLE 1. Effects of inhibitors on the reduction of MC and the formation of the alkylated complex of PNBP**

| | Reduction* (nmol/min/nmol nNOS) | Alkylation† (% of control) |
|---|---|---|
| Control‡ | 328 ± 21 | 100 |
| 1 mM KCN | 315 ± 18 | 93 |
| 1 mM L-NAME | 308 ± 23 | 89 |
| 50 μM DPI | 119 ± 11§ | 41§ |
| 100 μM DPI | 11 ± 3¶ | 8¶ |

* Reduction of MC was measured as the decrease in absorbance at 375 nm. The extinction coefficient of 13.2 $mM^{-1}$ $cm^{-1}$ was used to calculate the reduced MC content. Values are means ± SEM of three separate determinations.

† Alkylation refers to the formation of the alkylated complex of PNBP. The control value was 2.34 ± 0.13 $A_{540nm}$/min/nmol nNOS × $10^{-2}$.

‡ The control reaction mixtures consisted of 50 μM MC, 20 μM NADPH, and 0.0125 nmol nNOS for the reduction assay, and 3 mM NADPH, 0.1% PNPB, 0.3 mM MC, and 0.075 nmol nNOS for the alkylation assay, and the incubations were performed in 10 mM potassium phosphate, pH 6.6, under anaerobic conditions.

§ Significantly different ($P < 0.05$) from control.

¶ Significantly different ($P < 0.01$) from control.

reduction progressed well under anaerobic conditions. However, under aerobic conditions, MC reduction reached a maximum within 30 sec, and only 5% of MC was reduced. The rate of MC reduction was dependent on the concentration of nNOS (Fig. 2B). In the presence of the pre-boiled enzyme, MC remained unaffected and its reduction was not observed. The rate of MC reduction for the initial 3 min was proportional to the concentration of MC. However, MC saturation was not reached at concentrations up to 100 μM. nNOS exhibits a bidomain structure comprising a C-terminal reductase domain and an N-terminal oxygenase domain. To further confirm which domain was responsible for the reduction of MC, MC reduction was examined with inhibitors for both the oxygenase and reductase domains. As shown in Table 1, the nNOS competitive inhibitor L-NAME, which binds to the oxygenase domain, did not inhibit MC reduction at 1 mM. The heme blocker potassium cyanide, up to 1 mM, also did not affect MC reduction. In contrast, DPI, which binds to the reductase domain of nNOS, inhibited MC reduction in a concentration-dependent manner. At 50 μM DPI, the reduction of MC was inhibited by 64%, and it was inhibited completely at 100 μM. The reduction of MC by nNOS was influenced by $Ca^{2+}$/calmodulin. In the absence of $Ca^{2+}$/calmodulin, the rate of MC reduction decreased by 28% at pH 6.6 (Fig. 3).

### *Alkylation of PNBP by MC Metabolites*

To determine whether or not MC was converted to reactive metabolites that could bind covalently to macromolecules, the formation of an alkylated complex of PNBP produced by activated MC during incubation was measured. The formation of the alkylated PNBP adduct was linear with respect to the incubation time and to the MC and nNOS concentrations, in manners analogous to those observed in MC metabolic experiments. The results obtained for both

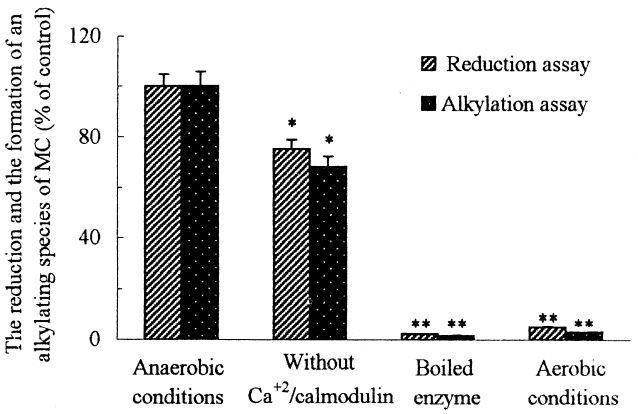


**FIG. 3. Comparative measurement of the reduction of MC by nNOS and the formation of the alkylated complex of PNBP by activated MC. Studies were conducted as described in Materials and Methods. Reaction mixtures contained 50 μM MC, 20 μM NADPH, and 0.0125 nmol nNOS for the reduction assay, and 3 mM NADPH, 0.1% PNPB, 0.3 mM MC, and 0.075 nmol nNOS for the alkylation assay, and the incubation was performed in 10 mM potassium phosphate, pH 6.6. Under anaerobic conditions, the values for the reduction of MC and the formation of the alkylated complex of PNBP were 328 ± 21 nmol/min/nmol nNOS and 2.34 ± 0.13 $A_{540nm}$/min/nmol nNOS × $10^{-2}$, respectively. The values under anaerobic conditions were regarded as the control. Data are expressed as means ± SEM for six independent experiments. Key: (*) $P < 0.05$, and (**) $P < 0.01$ compared with the group under anaerobic conditions.**

the reduction of MC and the alkylation of PNBP are shown in Fig. 3. With an aerobic atmosphere or pre-boiled enzyme, both the reduction of MC and the formation of the alkylated PNBP adduct were abolished. In the absence of $Ca^{2+}$/calmodulin, the formation of the alkylated PNBP adduct was reduced by 32%. The heme blocker potassium cyanide and the nNOS competitive inhibitor l-NAME did not affect the formation of the alkylated PNBP adduct, whereas DPI completely inhibited the formation of the alkylated PNBP adduct (Table 1).

### *Effect of pH on MC Reduction and Alkylation of PNBP*

The reduction of MC and the formation of the alkylated PNBP adduct were dependent on pH. As shown in Table 2, no significant decrease in nNOS activity from pH 7.6 to 6.6 was observed. nNOS-mediated cytochrome *c* reduction at pH 6.6 was increased by 15% as compared with that at pH 7.6 ($P > 0.05$). On the other hand, the rate of MC reduction and the formation of the alkylated PNBP adduct under anaerobic conditions at pH 6.6 were increased by 43 and 54%, respectively, as compared with that at pH 7.6 ($P < 0.05$).

### *Oxygen Consumption by nNOS-Catalyzed MC Reduction*

The reduction of MC by nNOS in air resulted in the consumption of oxygen. In the absence of MC, oxygen

**TABLE 2. Effects of pH on nNOS activity and MC metabolism**

| | nNOS activity (nmol/min/mg) | Cytochrome c reduction (μmol/min/nmol) | MC reduction (nmol/min/nmol) | Alkylation ($A_{540nm}$/min/nmol × $10^{-2}$) |
|---|---|---|---|---|
| pH 7.6 | 320 ± 17 | 11.4 ± 0.5 | 227 ± 18 | 1.52 ± 0.15 |
| pH 6.6 | 308 ± 14 | 13.1 ± 0.6 | 328 ± 21* | 2.34 ± 0.13* |

Values are means ± SEM of six separate determinations.
* Significantly different ($P < 0.05$) from values for corresponding reactions at pH 7.6.

consumption was low. However, a concentration-dependent increase in oxygen consumption with respect to the MC concentration was observed (Fig. 4A). The rate of oxygen consumption decreased by 50% in the presence of 2000 U/mL of catalase (Fig. 4B), indicating that oxygen was converted to hydrogen peroxide during MC reduction. One hundred micromolar DPI inhibited oxygen consumption completely, whereas the heme blocker potassium cyanide (1 mM) and the nNOS competitive inhibitor L-NAME (1 mM) did not affect oxygen consumption (Fig. 4B).

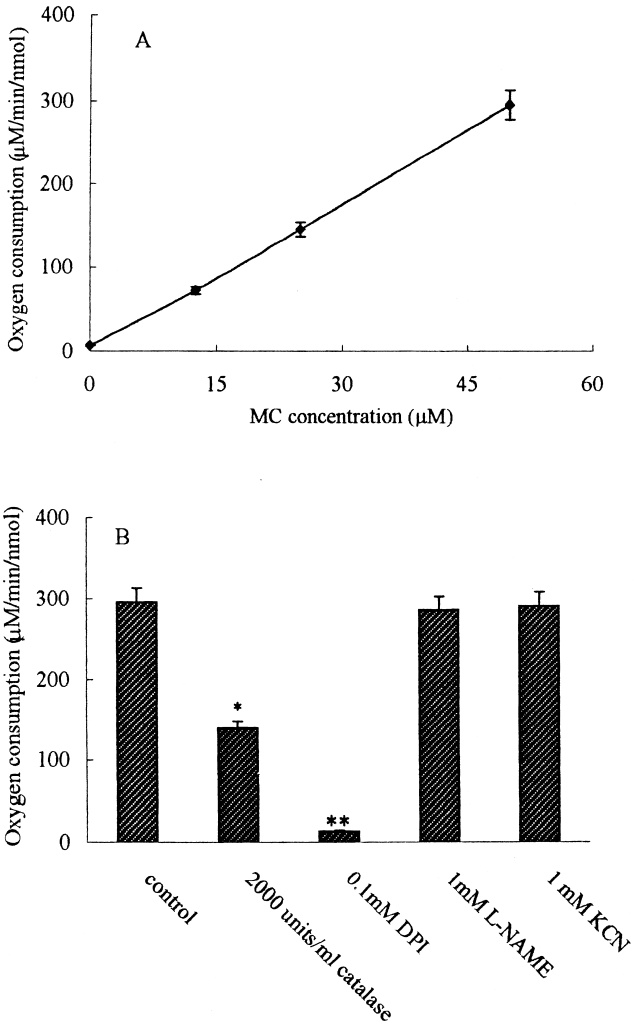


**FIG. 4. Oxygen consumption by nNOS-activated MC. (A) MC concentration-dependent oxygen consumption. The reactions were performed as described in Materials and Methods. (B) Effects of catalase, L-NAME, potassium cyanide, and DPI on MC-mediated oxygen consumption. Oxygen consumption was determined in the presence of 0.1 nmol nNOS, 50 μM MC (control), and 2000 U/mL of catalase, 1 mM L-NAME, 1 mM potassium cyanide, or 0.1 mM DPI. Data are expressed as means ± SEM for six independent experiments. Key: (*) $P < 0.05$, and (**) $P < 0.01$ compared with control.**

### *Inhibition of nNOS Activity by MC*

The reduction of MC catalyzed by nNOS suggested that MC binds to the reductase domain of the nNOS and inhibits the normal electron flow. To assess this hypothesis, nNOS activity was determined. Expectedly, MC inhibited both NO and L-citrulline (data not shown) formation in a concentration-dependent manner. The kinetic data for NO synthesis were plotted by the Lineweaver–Burk method, which showed that the inhibition of nNOS activity by MC was noncompetitive (Fig. 5).

## DISCUSSION

MC is considered to be the prototype bioreductive alkylating agent used in cancer chemotherapy. Reductive activation of MC is required for the generation of alkylating moieties [2]. NADPH-cytochrome P450 oxidoreductase [3, 4], xanthine oxidase [3, 5], cytochrome $b_5$ reductase [6],

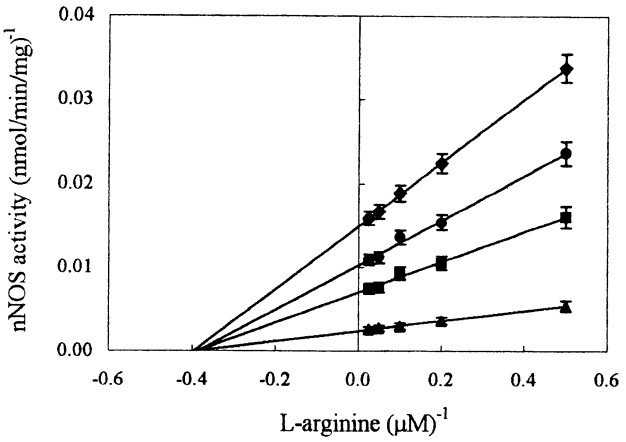


**FIG. 5. Double-reciprocal plots of the inhibition of nNOS activity by MC. nNOS activity was measured as described in Materials and Methods. Inhibition with respect to L-arginine is illustrated for MC at concentrations of 0 (triangles), 2.5 (squares), 5 (circles), and 10 μM (diamonds), while L-arginine varied from 2 to 40 μM. Data are expressed as means ± SEM for six independent experiments.**

xanthine dehydrogenase [7, 8], and DT-diaphorase [9] all have been identified as being capable of bioreducing MC to reactive metabolites. These enzymes activate MC, differing in their mechanisms, as well as in the resultant metabolites. However, more recent studies have shown that other undetermined enzymes must be involved in the metabolic activation of MC [11–14]. In this study, we showed that nNOS is capable of catalyzing the bioreduction of MC to generate reactive oxygen species and bioactive metabolites under aerobic and anaerobic conditions, respectively. MC uncouples the reductase domain of nNOS and shunts the electron away from the normal catalytic pathway, thus inhibiting nNOS activity.

NOS isoforms have a bidomain structure consisting of an oxygenase domain and a reductase domain. The reductase domain of NOS isoforms structurally resembles that of NADPH-cytochrome P450 reductase, having conserved binding sites for FAD, FMN, and NADPH [19]. Subsequent studies have demonstrated that this domain transfers NADPH-derived electrons either to an internal heme group located within the oxygenase domain of the enzyme or to an external heme protein acceptor, and thus it was suggested to participate in the cellular electron transfer process [29]. Herein, we showed that nNOS is capable of catalyzing the reduction of MC, which was measured as the decrease in absorbance at 375 nm. Under aerobic conditions, only 5% of MC was reduced, and the reduced MC did not accumulate indefinitely, suggesting that the overall extent of reduction represents the balance between the rate of MC reduction and the rate of reoxidation. In support of this explanation, nNOS completely reduced MC, and the reduced MC was maintained at a steady-state level under anaerobic conditions. Although it has been reported that nNOS catalyzes the generation of superoxide in the absence of L-arginine and $BH_4$ [36], the oxygen consumption was very low in the absence of MC. On the other hand, in the presence of MC, a concentration-dependent increase in oxygen consumption was observed, suggesting that the consumption of oxygen was induced by nNOS-catalyzed MC reduction, and not by nNOS itself. Taking into consideration the interaction of MC with other one-electron reductases, it is plausible that nNOS catalyzes a one-electron reduction of MC to the semiquinone radical intermediate under aerobic conditions. This intermediate undergoes redox cycles, regenerates the parent molecule, and reduces oxygen to generate superoxide, leading to oxygen consumption. Thus, hydrogen peroxide was formed by the spontaneous dismutation of superoxide, which was further confirmed by the observation that the rate of oxygen consumption was decreased by the addition of catalase. Under anaerobic conditions, the formation of the alkylated PNBP adduct paralleled the reduction of MC, indicating that bioactive metabolites of MC were generated. In the absence of oxygen, the one-electron metabolite of MC (semiquinone) chemically rearranges into the more stable hydroquinone, which probably serves as a common intermediate in both one- and two-electron reduction [37]. Upon reduction, the MC C-9a methoxy group is eliminated from the parent mitosane molecule, resulting in the formation of reduced mitosene intermediates displaying the characteristic double bond between the C-9a and C-9 positions of the molecule [38]. At this point, a number of different reaction schemes leading ultimately to DNA covalent modification have been hypothesized [1]. Only recently has it been clarified that three competing activation pathways yield three different DNA-reactive electrophiles, which generate three unique sets of DNA adducts as end products [39]. In the light of these results, it is concluded that nNOS is capable of catalyzing the reduction of MC to generate reactive oxygen species and bioactive metabolites under aerobic and anaerobic conditions, respectively.

Neither the heme blocker potassium cyanide nor the nNOS competitive inhibitor L-NAME, both of which bind to the oxygenase domain of nNOS, affected the MC-mediated oxygen consumption in air or inhibited the reduction of MC and the formation of the alkylated PNBP adduct under anaerobic conditions. These results indicated that the oxygenase domain of nNOS is not involved in the metabolic activation of MC. In contrast, the reductase domain inhibitor DPI completely inhibited the MC-mediated oxygen consumption in air, and the reduction of MC and the formation of the alkylated PNBP adduct under anaerobic conditions, demonstrating that the reductase domain of nNOS is responsible for the MC bioreduction. Calmodulin binding to nNOS not only triggers interdomain electron transfer between the reductase and oxygenase domains of nNOS, but also increases the rate of electron transfer to a variety of exogenous acceptors [21, 29]. Expectedly, $Ca^{2+}$/calmodulin enhanced the rate of MC reduction and the formation of the alkylated PNBP adduct.

The rate of MC reduction and the formation of the alkylated PNBP adduct were dependent on pH. No significant difference in nNOS activity between pH 7.6 and 6.6 was observed, nNOS-mediated cytochrome *c* reduction at pH 6.6 being increased by 15% as compared with that at pH 7.6. Consistent with our observation, recent studies have shown that the pH optimum for nNOS activity is between 7.0 and 7.5, with sharp decreases in activity below pH 6.5 and above pH 8.0, whereas nNOS-mediated NADPH oxidation increases at a pH below 7.0 [40]. The rate of MC reduction and the formation of the alkylated PNBP adduct under anaerobic conditions were increased by 43 and 54%, respectively, as the pH was decreased from 7.6 to 6.6, indicating that slightly acidic conditions facilitated the bioactivation of MC by nNOS. The acidic activation of MC without enzymatic reduction has been reported [41]. It is conceivable that the acidic activation of MC may account for at least part of the pH-dependent effect of MC bioactivation by nNOS.

MC inhibited nNOS activity in a noncompetitive manner, constituting further evidence that the reductase domain, but not the oxygenase domain, of nNOS is responsible for the reduction of MC. The binding of MC to the

reductase domain of nNOS diverts electron flow from the normal catalytic pathway. It is plausible that, with increasing MC concentrations, nNOS is transferred from a nitric oxide synthase to an NADPH oxidase.

Given the similar structures and mechanisms of the neuronal, endothelial, and inducible nitric oxide synthases, it is likely that all these isoforms catalyze MC bioactivation in a similar manner. Three NOS isoforms have been shown to be expressed in human central nervous system tumors [25], colon adenomas [26], and breast and ovarian tumors [27, 28]. Taking into consideration that increased toxicity of bioreductive MC under hypoxia in tumors is mediated presumably by one-electron reductases [12], it is postulated that, in addition to NADPH-cytochrome P450 reductase, xanthine oxidase, and cytochrome $b_5$ reductase, NOS isoforms are involved in MC bioactivation under anaerobic conditions *in vivo*.

Overexpression of NOS isoforms in tumors increases NO production, which is involved in the pathogenesis of cancer. A high concentration of NO has been shown to enhance tumor growth by increasing tumor blood flow, and to accelerate tumor growth of p53 mutant cells by inducing vascular endothelial growth factor expression and neovascularization [42]. The major thrust in the therapy of solid tumors is to prevent the development of new blood vessels, thus restricting solid tumor growth and causing the tumor to shrink. Inhibition of NO synthesis might also contribute to the antitumor activity of MC. More recently, the lack of a correlation *in vivo* between reductase enzyme expression, MC metabolic activation, and antitumor activity has been identified [1, 43], indicating that factors other than primary DNA damage may be more critical in our understanding of the determinants of the antitumor activity of MC. Herein, we showed that MC inhibits nNOS activity in a noncompetitive manner, suggesting the potential correlation of the inhibition of NOS activity and the antitumor activation of MC.

The findings presented here indicate that nNOS is capable of catalyzing the bioreduction of MC. The reduction of MC by nNOS generated reactive oxygen species and active metabolites under aerobic and anaerobic conditions, respectively. MC uncoupled the reductase domain of nNOS and shunted electrons away from the normal catalytic pathway, thus inhibiting nNOS activity in a noncompetitive manner. Additional studies are necessary to elucidate the potential correlation between NOS expression and MC metabolism in tumors, and whether or not the inhibition of NO synthesis contributes to the antitumor activity of MC *in vivo*.

## References


1. Cummings J, Spanswick VJ, Tomasz M and Smyth JF, Enzymology of mitomycin C metabolic activation in tumour tissue. *Biochem Pharmacol* **56:** 405–414, 1998.
2. Sartorelli AC, Hodnick WF, Belcourt MF, Tomasz M, Haffty B, Fisher JJ and Rockwell S, Mitomycin C: A prototype bioreductive agent. *Oncol Res* **6:** 501–508, 1994.
3. Pan S, Andrews PA, Glover CJ and Bachur NR, Reductive activation of mitomycin C and mitomycin C metabolites catalyzed by NADPH-cytochrome P-450 reductase and xanthine oxidase. *J Biol Chem* **259:** 959–966, 1984.
4. Keyes SR, Fracasso PM, Heimbrook DC, Rockwell S, Sligar SG and Sartorelli AC, Role of NADPH, cytochrome *c* reductase and DT-diaphorase in the biotransformation of mitomycin C. *Cancer Res* **44:** 5638–5643, 1984.
5. Tomasz M, Chowdary D, Lipman R, Shimotakahara S, Veiro D, Walker V and Verdine GL, Reaction of DNA with chemically or enzymatically activated mitomycin C: Isolation and structure of the major covalent adduct. *Proc Natl Acad Sci USA* **83:** 6702–6706, 1986.
6. Hodnick WF and Sartorelli AC, Reductive activation of mitomycin C by NADH:cytochrome $b_5$ reductase. *Cancer Res* **53:** 4907–4912, 1993.
7. Gustafson DL and Pritsos CA, Bioactivation of mitomycin C by xanthine dehydrogenase from EMT6 mouse mammary carcinoma tumors. *J Natl Cancer Inst* **84:** 1180–1185, 1992.
8. Gustafson DL and Pritsos CA, Kinetics and mechanism of mitomycin C bioactivation by xanthine dehydrogenase under aerobic and anaerobic conditions. *Cancer Res* **53:** 5470–5474, 1993.
9. Siegel D, Gibson NW, Preusch PC and Ross D, Metabolism of mitomycin C by DT-diaphorase: Role in mitomycin C-induced DNA damage and cytotoxicity in human colon carcinoma cells. *Cancer Res* **50:** 7483–7489, 1990.
10. Kennedy KA, Rockwell S and Sartorelli AC, Preferential activation of mitomycin C to cytotoxic metabolites by hypoxic tumor cells. *Cancer Res* **40:** 2356–2360, 1980.
11. Nishiyama M, Saeki S, Aogi K, Hirabayashi N and Toge T, Relevance of DT-diaphorase activity to mitomycin C (MMC) efficacy on human cancer cells: Differences in *in vitro* and *in vivo* systems. *Int J Cancer* **53:** 1013–1016, 1993.
12. Ross D, Beall HD, Siegel D, Traver RD and Gustafson DL, Enzymology of bioreductive drug activation. *Br J Cancer* **74** (Suppl XXVII)**:** S1–S8, 1996.
13. Joseph P, Xu Y and Jaiswal AK, Non-enzymatic and enzymatic activation of mitomycin C: Identification of a unique cytosolic activity. *Int J Cancer* **65:** 263–267, 1996.
14. Spanswick VJ, Cummings J and Smyth JF, Enzymology of mitomycin C metabolic activation in tumor tissue: Characterization of a novel mitochondrial reductase. *Biochem Pharmacol* **51:** 1623–1630, 1996.
15. Marletta MA, Nitric oxide synthase structure and mechanism. *J Biol Chem* **268:** 12231–12234, 1993.
16. Bredt DS and Snyder SH, Isolation of nitric oxide synthase, a calmodulin-requiring enzyme. *Proc Natl Acad Sci USA* **87:** 682–685, 1990.
17. Pollock JS, Nakane M, Buttery LK, Martinez A, Springall D, Polak JM, Forstermann U and Murad F, Characterization of and localization of endothelial nitric oxide synthase using specific monoclonal antibodies. *Am J Physiol* **265:** C1379–C1387, 1993.
18. Forstermann U, Gath I, Schwarz P, Closs EI and Kleinert H, Isoforms of nitric oxide synthase. Properties, cellular distribution and expressional control. *Biochem Pharmacol* **50:** 1321–1332, 1995.
19. Bredt DS, Hwang PM, Glatt CE, Lowenstein C, Reed RR and Snyder SH, Cloned and expressed nitric oxide synthase structurally resembles cytochrome P-450 reductase. *Nature* **351:** 714–718, 1991.
20. Sheta EA, McMillan K and Masters BSS, Evidence for a bidomain structure of constitutive cerebellar nitric oxide synthase. *J Biol Chem* **269:** 15147–15153, 1994.
21. Abu-Soud HM, Yoho LL and Stuehr DJ, Calmodulin controls neuronal nitric-oxide synthase by a dual mechanism. Activation of intra- and interdomain electron transfer. *J Biol Chem* **269:** 32047–32050, 1994.

22. Forstmann U, Gorsky LD, Pollock JS, Ishii K, Schmidt HHHW, Heller M and Murad F, Hormone-induced biosynthesis of endothelium-derived relaxing factor/nitric oxide-like material in N1E-115 neuroblastoma cells requires calcium and calmodulin. *Mol Pharmacol* **38:** 7–13, 1990.
23. Jenkins DC, Charles IG, Baylis SA, Lelchuk R, Radomski MW and Moncada S, Human colon cancer cell lines show a diverse pattern of nitric oxide synthase expression and nitric oxide generation. *Br J Cancer* **70:** 847–849, 1994.
24. Werner-Felmayer G, Werner E, Fuchs D, Hausen A, Mayer B, Reibnegger G, Weiss G and Wachter H, $Ca^{2+}$/calmodulin-dependent nitric oxide synthase activity in the human cervix carcinoma cell line ME-180. *Biochem J* **289:** 357–361, 1993.
25. Cobbs CS, Brenman JE, Aldape KD, Bredt DS and Israel MA, Expression of nitric oxide synthase in human central nervous system tumors. *Cancer Res* **55:** 727–730, 1995.
26. Ambs S, Merriam WG, Bennett WP, Felley-Bosco E, Ogunfusika MO, Oser SM, Klein S, Shields PG, Billiar TR and Harris CC, Frequent nitric oxide synthase-2 expression in human colon adenomas: Implication for tumor angiogenesis and colon cancer progression. *Cancer Res* **58:** 334–341, 1998.
27. Thomsen LL, Miles DW, Happerfield L, Bobrow LG, Knowles RG and Moncada S, Nitric oxide synthase activity in human breast cancer. *Br J Cancer* **72:** 41–44, 1995.
28. Thomsen LL, Sargent JM, Williamson CJ and Elgie AW, Nitric oxide synthase activity in fresh cells from ovarian tumour tissue: Relationship of enzyme activity with clinical parameters of patients with ovarian cancer. *Biochem Pharmacol* **56:** 1365–1370, 1998.
29. Klatt P, Heinzel B, John M, Kastner M, Böhme E and Mayer B, $Ca^{2+}$/calmodulin-dependent cytochrome *c* reductase activity of brain nitric oxide synthase. *J Biol Chem* **267:** 11374–11378, 1992.
30. Jiang HB and Ichikawa Y, Neuronal nitric oxide synthase catalyzes the reduction of 7-ethoxyresorufin. *Life Sci* **65:** 1257–1261, 1999.
31. Ogura T, Yokoyama T, Fujisawa H, Kurashima Y and Esumi H, Structural diversity of neuronal nitric oxide synthase mRNA in the nervous system. *Biochem Biophys Res Commun* **193:** 1014–1022, 1993.
32. Feelisch M and Noack EA, Correlation between nitric oxide formation during degradation of organic nitrates and activation of guanylate cyclase. *Eur J Pharmacol* **139:** 19–30, 1987.
33. Baek KJ, Thiel BA, Lucas S and Stuehr DJ, Macrophage nitric oxide synthase subunits. *J Biol Chem* **268:** 21120–21129, 1993.
34. Belcourt MF, Hodnick WF, Rockwell S and Sartorelli AC, The intracellular location of NADH:cytochrome $b_5$ reductase modulates the cytotoxicity of the mitomycins to Chinese hamster ovary cells. *J Biol Chem* **273:** 8875–8881, 1998.
35. McMillan K and Masters BSS, Prokaryotic expression of the heme- and flavin-binding domains of rat neuronal nitric oxide synthase as distinct polypeptides: Identification of the heme-binding proximal thiolate ligand as cysteine-415. *Biochemistry* **34:** 3686–3693, 1995.
36. Pou S, Pou WS, Bredt DS, Snyder SH and Rosen GM, Generation of superoxide by purified brain nitric oxide synthase. *J Biol Chem* **267:** 24173–24176, 1992.
37. Hoey BM, Butler J and Swallow AJ, Reductive activation of mitomycin C. *Biochemistry* **27:** 2608–2614, 1988.
38. Moore HW, Bioactivation as a model for drug design bioreductive alkylation. *Science* **197:** 527–532, 1977.
39. Suresh Kumar G, Lipman R, Cummings J and Tomasz M, Mitomycin C-DNA adducts generated by DT-diaphorase. Revised mechanism of the enzymatic reductive activation of mitomycin C. *Biochemistry* **36:** 14128–14136, 1997.
40. Gorren ACF, Schrammel A, Schmidt K and Mayer B, Effects of pH on the structure and function of neuronal nitric oxide synthase. *Biochem J* **331:** 801–807, 1998.
41. Tomasz M and Lipman R, Alkylation reactions of mitomycin C at acid pH. *J Am Chem Soc* **101:** 6063–6067, 1979.
42. Ambs S, Merriam WG, Ogunfusika MO, Bennett WP, Ishibe N, Hussain SP, Tzeng EE, Geller DA, Billiar TR and Harris CC, p53 and vascular endothelial growth factor regulate tumor growth of NOS2-expressing human carcinoma cells. *Nat Med* **4:** 1371–1376, 1998.
43. Spanswick VJ, Cummings J, Ritchie AA and Smyth JF, Pharmacological determinants of the antitumour activity of mitomycin C. *Biochem Pharmacol* **56:** 1497–1503, 1998.